Hydroxide Transport and Chemical Degradation in Anion Exchange Membranes: A Combined Reactive and Non-reactive Molecular Simulation Study

Journal:	*Journal of Materials Chemistry A*
Manuscript ID	TA-ART-11-2018-010651.R1
Article Type:	Paper
Date Submitted by the Author:	30-Jan-2019
Complete List of Authors:	ZHANG, Weiwei; Pennsylvania State University, Dong, Dengpan; University of Utah, Materials Science and Engineering Bedrov, Dmitry ; University of Utah, Materials Science & Engineering van Duin, Adri; The Pennsylvania State University, Mechanical and Nuclear Engineering

SCHOLARONE™
Manuscripts

Hydroxide Transport and Chemical Degradation in Anion Exchange Membranes: A Combined Reactive and Non-reactive Molecular Simulation Study

Weiwei Zhang[a], Dengpan Dong[b], Dmitry Bedrov[b*], and Adri C. T. van Duin[a*]

[a]Department of Mechanical and Nuclear Engineering, Pennsylvania State University, University Park, Pennsylvania 16802, United States. *Email: acv13@psu.edu

[b]Department of Materials Science and Engineering, University of Utah, Salt Lake City, Utah 84112, United States. *Email: d.bedrov@utah.edu

Abstract

Investigating the structural and dynamical properties, charge transport and membrane degradation in anion exchange membranes (AEMs) using atomistic-scale simulations provides a guideline in the design of new high-performance membrane fuel cells. In this work, we demonstrate a multiscale simulation strategy that combines molecular dynamics simulations using the non-reactive polarizable (APPLE&P) and reactive (ReaxFF) force fields. From the comparison of APPLE&P and ReaxFF results for four model AEMs with different functionalized groups, we show the importance of the Grotthuss mechanism for the OH^- diffusion, as well as for water self-diffusion in high OH^- concentration environments. With the incorporation of proton hopping in ReaxFF, the OH^- diffuses much easier through bottlenecks in the water channels, without losing some coordinating

water molecules. Furthermore, investigation of chemical degradation selectivity in different membranes with ReaxFF indicates that AEMs with cations connecting to large hydrophobic groups have better chemical stability. Considering the balance of transport and stability properties of AEMs, we propose a potential candidate for high performance membranes.

1 Introduction

Anion exchange membranes (AEMs) have been proposed as a potential alternative to proton exchange membranes for an application in fuel cells and attracted widespread attention in the past two decades due to their ability to use the low cost of noble-metal-free electrodes.[1-4] However, the practical use of AEMs is still challenging because of their relatively low chemical stability in highly alkaline environments and at elevated temperatures.[5] It is known that the most common polymer-bound cation, the quaternary ammonium, undergoes a variety of chemical degradation pathways involving substitutions, Hofmann elimination and other rearrangements.[6-8] Therefore, improving the stability of AEM with prominent conductivity is an important target in the design of good-performance AEMs. Recent experimental studies indicate that membranes with long alkyl side chain have much better alkaline stability and sufficient long-term stability in fuel cell application compared to membranes with the short cationic side chains.[5, 9, 10] In consistence with experiments, the ReaxFF molecular dynamics (MD) simulation also showed that long hydrophobic alkyl side chain can prohibit the OH^- from approaching the cation center resulting in a lower degradation rate.[11]

By taking advantage of MD simulations coupled with high performance computing capabilities, the large-scale simulations provide more details in the material properties,

which can be very helpful in the design of novel AEMs with enhanced performance. However, there still remain some challenges in extracting such information from AEM simulations at nano scale level. One of such challenges is the conductivity prediction. The OH^- diffusion, the main charge carrier contributing to conductivity, involves both the Grotthuss hopping[12] and vehicular diffusion through water channels in AEMs.[13] Conventional classical MD simulation methods do not take the Grotthuss hopping into account and they thus can only sample the vehicular portion of OH^- diffusion.[11] *Ab initio* MD (AIMD) simulations have the ability to describe the proton hopping behavior, but significant computational cost limits the applications in very small systems at short time scales, which usually leads to poor sampling of different local environments/events that can occur in the AEM.[14, 15] As such, classical methods are still commonly used to study membrane microstructure and transport characteristics at nano scale. For instance, Zhuang group employed coarse-grained MD simulation to identify the optimal AEM from several candidate polymer structures and the results of their simulations showed good agreement with experimental observations.[16] Lu *et al.* recently studied the relationship between water activity and water content in polymer electrolyte membranes.[17] Several research groups have developed hybrid methods incorporating the proton hopping into traditional classical MD methods to study H_3O^+/OH^- diffusion. For example, Devanathan *et al.* employed quantum hopping (Q-HOP) MD simulation approach to consider the proton transport in the membrane.[18] Voth and coworkers applied multistate empirical valence bond (MS-EVB) approach to study AEMs and proton exchange membranes.[19, 20]

Another challenge in AEM simulations is the chemical degradation process of

membrane. As mentioned above, AEMs usually exhibit poor chemical stability in alkaline environments at high temperatures in comparison to proton exchange membranes and it is usually a detrimental issue limiting the performance and lifetime of AEMs.[21-23] However, most of simulation tools mentioned above cannot be employed to investigating the chemistry of membrane because they were developed on the basis of fixed connectivity of atoms, therefore not being able to describe the bond breaking and formation. For this reason, ReaxFF approach is more suitable to study the chemical aspects of proton transport and AEM chemical degradation. ReaxFF is a bond order dependent reactive force field, capable of simulating chemical reactions in large system ($> 10^6$ atoms at nanosecond time scale).[24, 25] It has been widely used to study the high-energy materials, metals/metal oxides and polymer decompositions in the gas and solid phases, as well as the chemical reaction at interface.[26-29] Our previous studies have shown the ReaxFF is indeed capable of predicting the proton transport and chemical degradation in AEMs.[11]

However, ReaxFF is still a relatively expensive method compared to traditional classical methods to simulate polymeric systems at large scale. Thus, in this work, we have combined the Atomistic Polarizable Potential for Liquids, Electrolytes, & Polymers (APPLE&P) classical polarizable force field and ReaxFF reactive force field to study a series of poly (p-phenylene oxide) (PPO) based AEMs, where the side chain is functionalized with different quaternary ammonium cationic groups. Simulation using the APPLE&P model has the ability to give better sampling of the system on long-time scales (e.g. microseconds). Recently, we have demonstrated that combination of the APPLE&P and ReaxFF simulations is an efficient way to investigate the Grotthuss mechanism transport in AEMs.[30] However, the balance between conductivity and

chemical stability is more crucial in the design of high performance AEMs. In this work, we therefore systematically studied the cationic side chain length effect on the structure, charge transport and chemical stability of model AEMs. It should be mentioned that structural and dynamic properties of degraded AEMs can also be studied by switching the ReaxFF back to APPLE&P MD simulation. With this alternating strategy, one can study the degradation effect on the phase segregation of membranes efficiently at a relatively larger length and sufficiently long-time scales.

On the basis of our combined APPLE&P and ReaxFF study of AEMs with different functional cationic groups and the comparison of the predicted membrane structure, hydroxide transport and chemical stabilities, we identify the most promising polymer functional group for the potential application in PPO-based AEM fuel cell. The novel simulation concept paves a new way towards the theoretical understanding and prediction of both physical and chemical properties of realistic polymer membrane electrolytes.

2 Computational Methods

2.1 Systems

In this work, we investigated four AEMs comprised of PPO chains functionalized with different cationic groups as shown in Figure 1. There are 16 chains in each system and each polymer chain contained 5 monomers (n=5 in Figure 1) with each monomer containing a hydrophobic and hydrophilic unit. For PPO-based AEMs the hydration levels (λ), defined as the ratio of water and hydroxide ions, are typically between 5 and 20 as reported in experimental literatures.[31, 32] It is known that too low water uptake often leads to low conductivity and poor chemical stability while too high water uptake results in high

dimensional swelling and low mechanical strengths of membrane electrode assemblies.[17] Therefore, in this work we investigated membranes with intermediate hydration level $\lambda=10$ which is consistent with typical experimentally functioning PPO-based membranes containing 80 hydroxide ions and 800 water molecules for each system. For the purpose of understanding the influence of water content on membrane characteristics, we also studied the PPO-3C1 and PPO-3C3 membranes with other hydration levels, such as $\lambda=5$ and 17.

PPO-3C1: $R_1=R_2=R_3=-CH_3$
PPO-2C1-C6: $R_1=R_2=-CH_3$, $R_3=-(CH_2)_5CH_3$
PPO-2C1-EO: $R_1=R_2=-CH_3$, $R_3=-(CH_2)_4OCH_3$
PPO-3C3: $R_1=R_2=R_3=-(CH_2)_2CH_3$
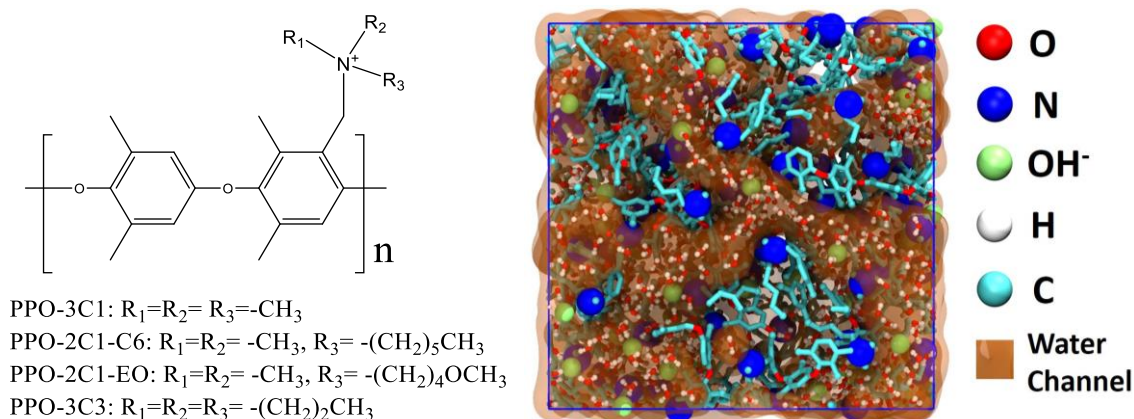
Figure 1: The chemical structures of PPO-3C1, PPO-2C1-C6, PPO-2C1-EO and PPO-3C3 (left panel). The backbones of all AEMs are the same and functional groups of R_1, R_2 and R_3 are different. A typical snapshot of simulation box (PPO-2C1-C6) is given in the right panel.

2.2 APPLE&P Polarizable Molecular Dynamics Simulations

The preparation of simulation systems utilizing APPLE&P force field was consistent with our recent study of PPO-based AEMs.[30] Initially, the polymer chains, hydroxide ions and water molecules were randomly placed inside a $300 \times 300 \times 300$ Å cubic box. The simulations box was shrunk over short MD simulation to dimensions expected for these

systems at 1 atm. and 298 K. Short simulations in the NPT ensemble were conducted to obtain stable simulation cell dimensions. Next simulations using annealing strategy was employed to accelerate polymer relaxation from various local minima and promote the migration of species for micro-phase segregation.[33, 34] In these simulations the systems were heated up to 2000 K in the NVT ensemble with a gradual change of temperature. At this elevated temperature, a 3 ns simulation run was conducted in the NVT ensemble to allow relaxation of polymer conformations and hydration structures. Within another 3 ns, the system was annealed to 298 K, followed by a 5 ns run in the NPT ensemble to equilibrate the system. Production runs in the NPT ensemble were subsequently conducted over 30 ns. In our recent study, we have demonstrated that the cooling rate shows rarely affect the polymer morphology and OH-anion/water dynamics.[35] For example, two more independent system realizations have been set up starting from random initial configurations in the large simulation box. But the resulting distributions of water channel dimensions and dynamical properties of species were very similar between different realizations as shown in Figures S10 and S11, respectively.

2.3 ReaxFF Reactive Molecular Dynamics Simulations

Generally, in order to prevent membrane degradation in the ReaxFF annealing procedure, OH^- anion has to be replaced by water molecule and then changed back to study the structural properties of real system at room temperature.[11] However, our recent APPLE&P study demonstrated that the polarization interactions significantly affect the hydration structure of water around hydrophobic polymers.[36] One thus expects that replacement of OH^- might change the local environment and possibly affect the structure of the hydrated AEMs. Performing ReaxFF MD simulation based on the configurations

sampled from long-term APPLE&P simulations allows us to avoid the annealing simulation in ReaxFF, as well as to lower computational cost. In this work, all ReaxFF simulations were run with the recently parameterized CHNO-2017_weak reactive force field potential, which showed good description of weak interactions of functionalized hydrocarbon/water in condensed phase as discussed elsewhere.[37] A 200 ps NPT/MD simulation at room temperature was first performed to equilibrate the density of system. After that, we performed a 1.0 ns NVT/MD simulation at 300 K and the data from the last 800 ps were used to obtain the reliable structural and dynamical properties. In the study of AEM degradation, the 250 ps simulations were run at 500 K, which is higher than typical experimental operation temperature (usually ~380 K[9]), to accelerate the degradation rate. The time step was set to 0.25 fs and the Berendsen thermostat was employed with pressure and temperature damping constant of 2500 and 100 fs for the NPT and NVT MD simulations, respectively. All ReaxFF simulations were carried out with ADF-2017 computational chemistry package.[38] It should be mentioned that the change of polymer conformation usually requires very long simulation times. However, we mainly focus on the hydroxide transport and chemical degradation at a particular morphology in this work. We believe that the strategy of switching between ReaxFF and APPLE&P MD simulations can provide a powerful way to study the polymer conformation effect on the membrane properties.

3 Results and Discussion

3.1 Mapping between ReaxFF and APPLE&P

Comparing the density is a straightforward criterion to evaluate the consistency between APPLE&P and ReaxFF force fields in the description of system thermodynamics.

The predicted densities at room temperature with two force fields are summarized in Table 1 for all investigated AEMs. The ReaxFF densities are in excellent agreement with the APPLE&P predictions (less than 1.0% deviation). Also, as expected, the higher water uptake leads to higher dimensional swelling of the membrane. For example, the volume for the PPO-3C1 membrane with $\lambda=17$ is about 24.8% larger than that with $\lambda=10$. Although, as our study demonstrated previously, the higher hydration level enhances the conductivity of membrane,[11] the membrane swelling usually causes low mechanical strength and difficulty in maintaining the *in situ* integrity of membrane electrode assemblies,[39, 40] both of which are undesirable for fuel cell applications.

Table 1. Comparison of densities (g/cm^3) predicted with APPLE&P and ReaxFF NPT/MD simulations at 300 K, respectively.

AEMs	APPLE&P	ReaxFF
PPO-3C1	1.159±0.005	1.166±0.002
PPO-2C1-C6	1.114±0.004	1.121±0.003
PPO-2C1-EO	1.145±0.004	1.145±0.001
PPO-3C3	1.113±0.004	1.109±0.001
PPO-3C1 ($\lambda=17$)	1.161±0.004	1.153±0.001
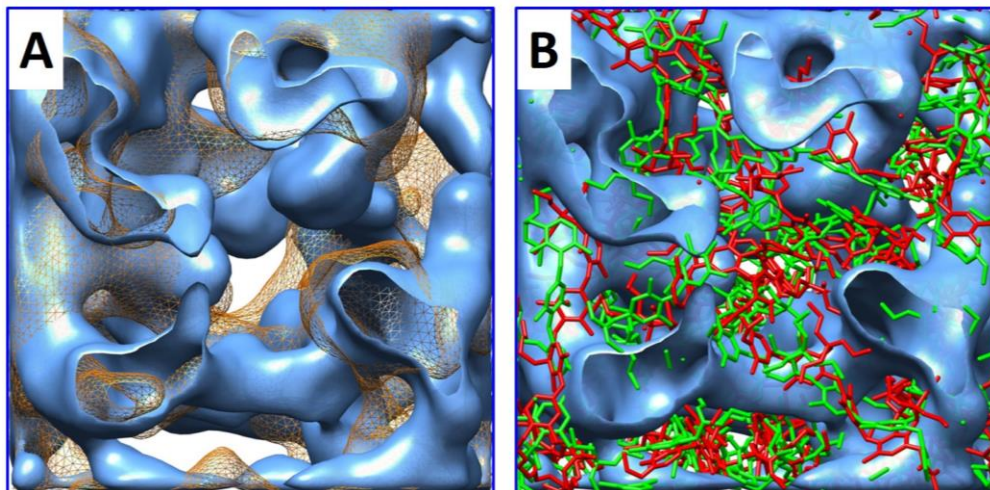
Figure 2: a) Water channels in PPO-3C3 membrane drawn at 50% of bulk water density (isosurface in solid representation obtained from APPLE&P simulations, wireframe representation after mapping and equilibration using ReaxFF). b) Comparison of the polymer phase, in which red and green skeletons are for the polymers from APPLE&P and after mapping to ReaxFF, respectively.

To visualize a comparison between membrane configurations simulated using the APPLE&P and ReaxFF models, a typical snapshot of an AEM is presented in Figure 2. We observe that the original APPLE&P predicted configuration is preserved very well after it is mapped to ReaxFF simulations. It indicates that the ReaxFF simulations preserve the phase segregated morphology of the hydrated membrane predicted by APPLE&P simulations. In addition, all polymer chains in ReaxFF and APPLE&P are aggregated locally and are separated by inter-connecting water channels. Our previous study has demonstrated the morphology of these AEMs is determined by the concentration of the amphiphilic polymer units. i.e., the hydrophilic and hydrophobic polymer segments are likely to self-assemble at low hydration level with water channels forming a bicontinuous network involving hydrophilic polymer segments.[35] A more

detailed comparison between ReaxFF and APPLE&P structures indicate some discrepancies between these models predictions. For instance, the water domain slightly expands further after ReaxFF NPT/MD simulations in PPO-3C3 AEM. Such expansion probably arises from the different interaction between the water molecules and polymers in the APPLE&P and ReaxFF, which can be confirmed by the discrepancy observed in the radial distribution functions (RDFs) of N-O(H_2O) as shown in Figure 3. For example, it is found the water molecule is closer to the cationic groups in ReaxFF than in APPLE&P, indicating the water-polymer has stronger attracting interaction within a short distance in ReaxFF. As a result, the water domain is expanded during ReaxFF simulations. Additionally, large fluctuations of cell volume at the initial simulation stage (see Figure S1) of the mapping and the thermal fluctuations of membrane with time evolution also might be the reason causing some changes in the morphology of water domains. In order to validate the mapping between two force-fields further, we also compared a selected polymer chain backbone and showed its configuration in Figure S3. It is clear that the overall chain conformation is preserved although a small local fluctuation of polymer segments is observed.

3.2 Structural Properties
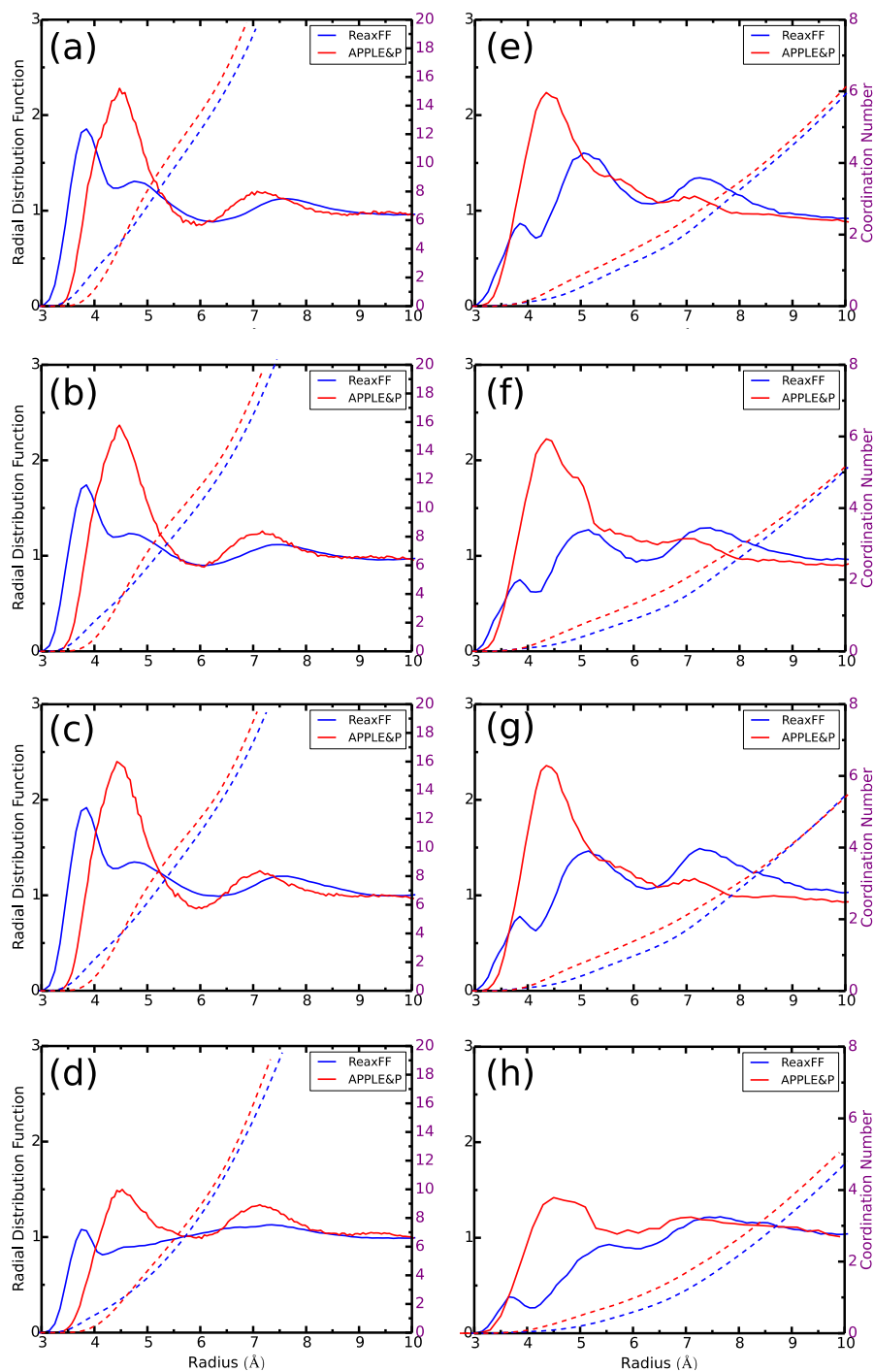
Figure 3: The RDFs and coordination numbers of N-O(H₂O)(left, a-d) and N-O*(OH⁻) (right e-h) for PPO-3C1, PPO-2C1-C6, PPO-2C1-EO and PPO-3C3 AEMs (from top to bottom) predicated with APPLE&P (red) and ReaxFF (blue), respectively.

Due to the fact that the chain conformation is well preserved after mapping from APPLE&P to ReaxFF and the fact that water and OH⁻ diffusion are primarily influenced by the quaternary ammonium cation hydration structure, we therefore mainly focused our structural analysis on the RDFs of N-O(H_2O) and N-O*(OH⁻) (nitrogen-oxygen of water and nitrogen-oxygen of hydroxide ion pairs, respectively). Figure 3 shows the RDFs of PPO-3C1, PPO-2C1-C6 and PPO-2C1-EO. It is clear that the RDF curves of N-O(H_2O) are similar to each other when simulated using the same force field, but the first RDF peak is much weaker in PPO-3C3 compared to other systems. This indicates that the three hydrophobic propyl groups reduce water accessibility to cationic groups in PPO-3C3. As a result, it shows a weak correlation between cation and water molecules. In addition, the RDFs of N-O*(OH⁻) are also displayed in Figure 3. Again, the correlation in PPO-3C3 is much weaker than in other systems because the larger alkyl groups push the OH⁻ anion further away from the cation center. Comparing the APPLE&P and ReaxFF results, we find the position of the first peak predicted by ReaxFF shifts to shorter distance by about 0.5 Å and the peak splits into two for the N-O (H_2O) RDFs in PPO-3C1, PPO-2C1-C6 and PPO-2C1-EO. One strong intensity peak is located at about 3.8 Å and a shoulder at around 4.8 Å. The first peaks of N-O*(OH⁻) RDFs predicted by ReaxFF are weaker than by the APPLE&P simulations, indicating weaker correlations for all membranes and more opportunity to find the OH⁻ away from cationic nitrogen. We expect that the RDF discrepancy of N-O(H_2O) and N-O*(OH⁻) predicted by two force field models comes from their different treatment of the electrostatic interactions and atom charge calculation methods. ReaxFF employs the geometry dependent Electron Equilibration Method (EEM), in which the charge is more delocalized for cation and OH⁻ compared to that in APPLE&P,

where the charge is geometry independent but the local polarization effects are included through point induced dipoles. In order to better understand this, we took a relative small system as an example (40 OH$^-$, 400H$_2$O and 40 trimethylamines attached to p-phenylene oxide dimer (TPO)) and run the simulation using constrained ReaxFF simulations, where we fixed the charge of cationic group to 1.0e and aromatic part to 0.0e for each organic molecule, while the total negative charge of -40.0e was assigned to all water molecules and OH$^-$ anions (assignment of the negative charge to each bare OH$^-$ is unfeasible due to the proton hopping between OH$^-$ and water molecules). The RDFs predicted with APPLE&P, standard ReaxFF, and charge constrained ReaxFF simulations are shown in Figure S5. As expected, all RDFs predicted by constrained ReaxFF show strong correlations at short distances compared to the standard ReaxFF simulation and move towards the APPLE&P result. Therefore, the difference in RDFs seen in Figure 3 indeed stems from the difference in electrostatic interactions. Most importantly, although the RDFs show some deviations, the morphology of the hydrated membranes are very similar to each other and the two MD methods predict the same water channel size distribution as discussed below. In addition, from Figure 3, we find APPLE&P and ReaxFF predict the similar coordination numbers (CNs), indicating the probabilities of OH-anion approaching the cationic group of polymers are same, which is related to the chemical degradation selectivity for different membranes.
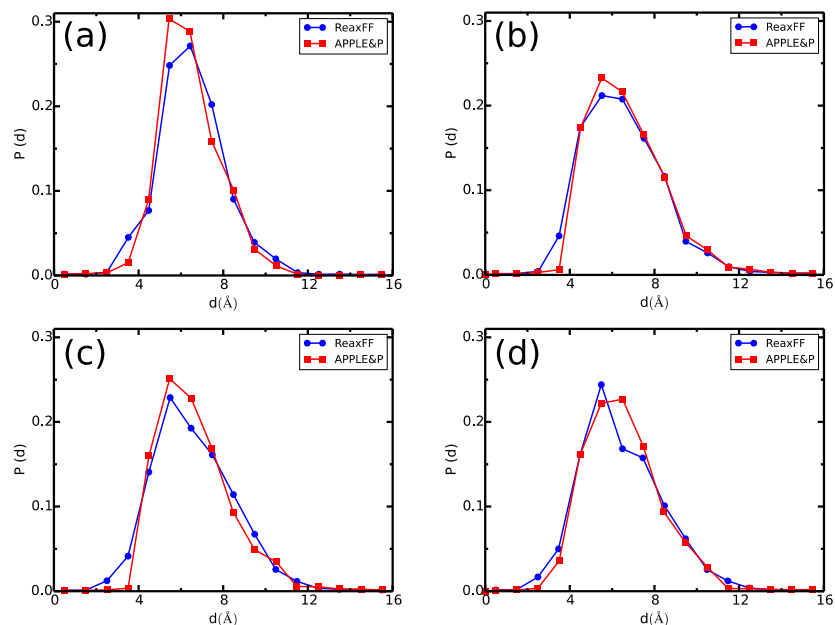
Figure 4: Water channel size distributions in PPO-3C1(a), PPO-2C1-C6(b), PPO-2C1-EO(c), and PPO-3C3(d) AEMs predicted with ReaxFF (blue) and APPLE&P (red), respectively.

To further compare the morphology of membrane predicted by two methods, in Figure 4 we show distribution of water channels size. The method to calculate the distribution of water channel sizes follows the method widely used in the analysis of 'pore-size-distribution',[41] and was modified accordingly for the analysis of PPO-based membranes.[30] Details of this analysis are described in the Supporting Information. Figure 4 illustrates that the change in morphology caused by the configurations mapping from the APPLE&P to ReaxFF is minimal, which reflects the difference in dynamics, without concerning about discrepancies in the structure of water channels.

From the comparison of density, morphology of polymer, RDF and water channel size distribution predicted by APPLE&P and ReaxFF simulations, we expect the direct mapping of AEM morphologies between two models to be effective and reliable.

Therefore, combining the reactive and nonreactive polarizable MD simulations is an efficient approach that allows us to appropriately investigate the Grotthuss mechanisms and the chemical properties of AEMs as discussed in the next sections.

3.3 Transport Properties

The water and OH^- diffusion is one of the most critical factors to assess the AEMs performance. Therefore, we calculated the diffusion coefficients of water and OH^- in four AEMs and listed the results in Table 2. Comparing the water diffusion constants predicted by APPLE&P and ReaxFF, we find the water diffusion simulated with ReaxFF is about five times larger than that calculated by APPLE&P, indicating the water becomes 'glassy' in non-reactive simulations. There are possible two reasons explaining the observed difference. One might be the difference in short-range interactions between water molecules and functionalized cation group. From the comparison of RDFs between APPLE&P and ReaxFF in Figure 3, it was observed that simulations with APPLE&P predict stronger water-cation correlations, potentially leading to the slower dynamics of water molecules. Another reason is the absence of the Grotthuss proton hopping in APPLE&P simulations. As shown in Table S2, the hydrogen bond (HB) lifetime of OH^--water is about factor of six longer than that in water-water. Therefore, in the case of high OH-concentration as in present systems, where more than 40% water molecules bonding to OH^- anions to form $OH\text{-}(H_2O)_n$ clusters due to the hyper-coordinated of OH^- (> 4), [42] the slow dynamics of $OH\text{-}(H_2O)_n$ will further lead to the slow diffusion of water overall. In contrast, the water dynamics becomes much faster in ReaxFF, because the hydrogen bond network is involved in rapid reorganization in ReaxFF due to the Grotthuss proton hopping. The high frequency disruption of the hydrogen bond network

leads to fast water diffusion and makes it much closer to the experiment measurement. For example, the water diffusion constant in copolymer [poly(2,6 dimethyl 1,4 phenylene oxide)-b-poly(vinyl benzyl trimethyl ammonium)] AEM can reach up to 0.07 Å^2/ps,[31] which is even higher than the present ReaxFF prediction. In addition, to understand the OH-anion effect on the water diffusion constant in ReaxFF, we compared the water diffusion constants in the PPO-3C3 AEM and that in the absence of OH-anion. It is interesting to find that water diffuses much faster (about twice as fast) in the AEM without OH^-, also indicating the stable HB in OH-water makes the water glassy to some extent in ReaxFF. From the above comparison, we conclude that both HB in OH-water and Grotthuss proton hopping can affect the water self-diffusion and the two factors show opposite contributions to the dynamics. Namely, the strong hydrogen bonding interaction between OH-anion and water molecules (APPLE&P, as well as ReaxFF) leads to the slow water dynamics, while the Grotthuss proton hopping in ReaxFF, which breaks the hydrogen bond network because of proton hopping, favors water diffusion. It should be mentioned that such competitive effects on the water dynamics may be prominent barely at the high alkaline concentration (i.e. low water uptake in AEMs).

In order to understand the importance of the Grotthuss proton hopping to the OH-anion diffusion, we calculated the D_{OH^-}/D_{H_2O} ratio and listed it in Table 2. We find the ratio is around 0.2 in APPLE&P, while there is opposite trend with the ratio up to 5.0 in ReaxFF. This indicates that Grotthuss hopping mechanism significantly enhances the dynamics of OH^- comparing to water. The lower ratio in APPLE&P is expected to arise from the synergistic diffusion of OH-anion and water molecules, leading to retarded diffusion of OH^- in sub-nanometer wide water channels, especially at the bottlenecks of

these water channels, where the OH⁻ has to lose its coordinating water molecules. In contrast, during the ReaxFF simulations, which includes the proton hopping, no significant loss of coordinating water was observed.[30] The smooth transition of OH⁻ through bottlenecks of water channels can be achieved by a series of proton hopping from water molecules to hydroxide anion. As a result, the D_{OH^-}/D_{H2O} ratio is obviously higher than that in non-reactive simulations, qualitatively consistent with experimental observations. As demonstrated in our previous work, the OH⁻ diffusivity significantly slows down when proton hopping in ReaxFF is "switched off".[30] In addition, considering the fact that the D_{OH^-}/D_{H2O} ratio in AEMs is much larger than that in pure bulk water,[42] it demonstrates that compared to bulk water case, the OH⁻ in AEMs becomes less-hydrated structure, resulting in larger proton hopping probability. Such findings are very helpful to design different cation structures with the improved chemical stability while simultaneously keeping the high conductivity.

Table 2. Comparison of diffusion constant ($Å^2$/ps) of water molecule and hydroxide ion at the room temperature, as well as OH⁻ and water ratios.

		PPO-3C1	PPO-2C1-C6	PPO-2C1-EO	PPO-3C3
D_{H2O}	APPLE&P	0.0058±0.0001	0.0083±0.0004	0.0064±0.0001	0.0063±0.0002
	ReaxFF	0.040±0.0008	0.041±0.0008	0.037±0.0010	0.033±0.0009
D_{OH^-}	APPLE&P	0.0012± 6.5×10^{-5}	0.0020± 5.4×10^{-5}	0.0014± 4.0×10^{-5}	0.0010± 1.3×10^{-4}
	ReaxFF	0.192±0.007	0.236±0.008	0.186±0.008	0.182±0.010
$D_{OH^-}/$ D_{H2O}	APPLE&P	0.21	0.24	0.22	0.16
	ReaxFF	4.57	5.90	4.90	4.91

Since the Grotthuss mechanism plays a very important role in the OH$^-$ diffusion, as well as the water self-diffusion, we study the relationship between diffusion constant and polymer structure, mainly focused on the analysis from the ReaxFF results. It can be seen from Table 2 that D_{OH^-} shows stronger dependence on the polymer structure than the D_{H2O}. For example, the diffusion constants of OH$^-$ are 0.236 Å^2/ps in PPO-2C1-C6, which is about 30% faster than that in PPO-3C3, while we see only an increase of 20% for the water diffusion. Considering the large contribution from Grotthuss mechanism, the hopping rate of OH$^-$ per unit time has thus been calculated and shown in Table S1. We found roughly identical hopping rates in all AEMs. One expects that the morphology of polymer membrane might play a role in determining the "efficiency" of Grotthuss hopping. In addition, our recent non-reactive simulations have demonstrated the OH$^-$ and water diffusion can be enhanced in the AEMs with co-existence of phase segregation and well-defined water channels compared to that in the AEMs with enhanced phase segregation and disconnection between neighboring water-rich domains (also see Supporting Information).[35] Similar findings are observed in our ReaxFF simulations. For example, the OH$^-$ and water diffusion constants in PPO-2C1-C6 are larger than that in PPO-3C3, even though the morphology dependence becomes weaker in ReaxFF compared to the APPLE&P simulations. Furthermore, from the comparison of diffusion constants of PPO-2C1-C6 and PPO-2C1-EO, which have the same size of cation groups, it is interesting to find that both water and OH$^-$ diffuse slower in PPO-2C1-EO than in PPO-2C1-C6. This indicates that the ether group, which is hydrophilic, might damage the well-defined water channel environment, appearing in PPO-2C1-C6. Knowing the OH$^-$ diffusion constant, the ionic conductivity can be estimated using Nernst-Einstein

19

equation.[43, 44] As shown in Table S3, it is clear that the ionic conductivity has the same trend as the diffusion constants for all four AEMs and the ReaxFF predicted ionic conductivity can be comparable with experimental measurement for other AEMs,[31, 45] while APPLE&P significantly underestimates it. Conclusively, although different mechanism has been observed in APPLE&P and ReaxFF, the trend of polymer morphology in determining transport efficiency of OH^-, either translational motion in APPLE&P or effective Grotthuss hopping in ReaxFF, is universal. Our results indicate that enhanced nano-phase segregation with well-defined water channels should be the key target in the design of membranes with high OH^- transport efficiency.

3.4 Degradation selectivity of AEMs

Chemical stability of AEMs limits the performance and lifetime of the AEMs. Understanding of degradation mechanism and degradation rate is thus critical to AEM design. In this work, we employed ReaxFF to explore the chemical stability of AEMs. Figure 5 shows four main possible pathways of degradation for PPO-2C1-C6 AEM in literature, namely methyl group losing (reaction 1), Hofmann elimination (reaction 2), entire cationic group losing (reaction 3), and backbone cleavage (reaction 4).[5, 46, 47] However, with the present ReaxFF simulation time scale and alkaline condition, only reactions 1 and 2 were observed. The reason might be that the reaction sites in pathways 3 and 4 are more hydrophobic and the $OH^-(H_2O)_n$ cluster is more likely to attack the hydrophilic reaction sites such as pathways 1 and 2. Consequently, the degradation paths involving the loss of whole cationic group and cleavage of backbone cannot be straightforwardly sampled with ReaxFF simulation at current simulation time scale.[11] Comparing reaction pathway 1 with 2, we observed the reaction of methyl group losing is

the main degradation pathway via multi-OH anion attack.[37] In detail, an OH^- approaches the cation and first abstracts hydrogen from $-CH_3$ group. As a result, the generated water molecule moves away and allows the second OH^- to attach the under-coordinated $-CH_2$ group and release its hydrogen towards the third OH^- molecule. Eventually, the bond breakage between nitrogen and carbon is observed due to the over-coordination of carbon and generate CH_2O formation. Such multi-OH anion attack reaction pathway seems to be more energetically favorable in aqueous solution than the S_N2 pathway,[37] the latter is proposed on the basis of the DFT calculations for very small systems with only one OH-anion attack.[7] Both reaction pathways lead to the similar chemistry. Pathway 2 is related to the Hofmann elimination, which is one of degradation pathways in the long alkyl side chain membranes observed in experiment.[5] According to our most recent study of chemical degradation pathways of tetramethylammonium,[37] we are aware that the reaction barriers predicted by ReaxFF are lower than DFT data, indicating that ReaxFF accelerates the chemical degradation rate. If ReaxFF reproduce the DFT-barriers, no chemical reaction can possibly happen within the regular MD accessible timescales (nanoseconds) as the reported degradation lifetime is from minutes to hundreds of hours in experiment. Generally, biased sampling methods, such as umbrella sampling, meta-dynamics, and bond-boost method, etc., are utilized to accelerate the reaction rates. The present ReaxFF is an alternative way to accelerate the chemistry events without switching the reaction rate order of different functional groups; we here seek to demonstrate that ReaxFF is reliable to study the chemical degradation selectivity for different membranes, which is very helpful in the design of high performance AEMs in experiment.
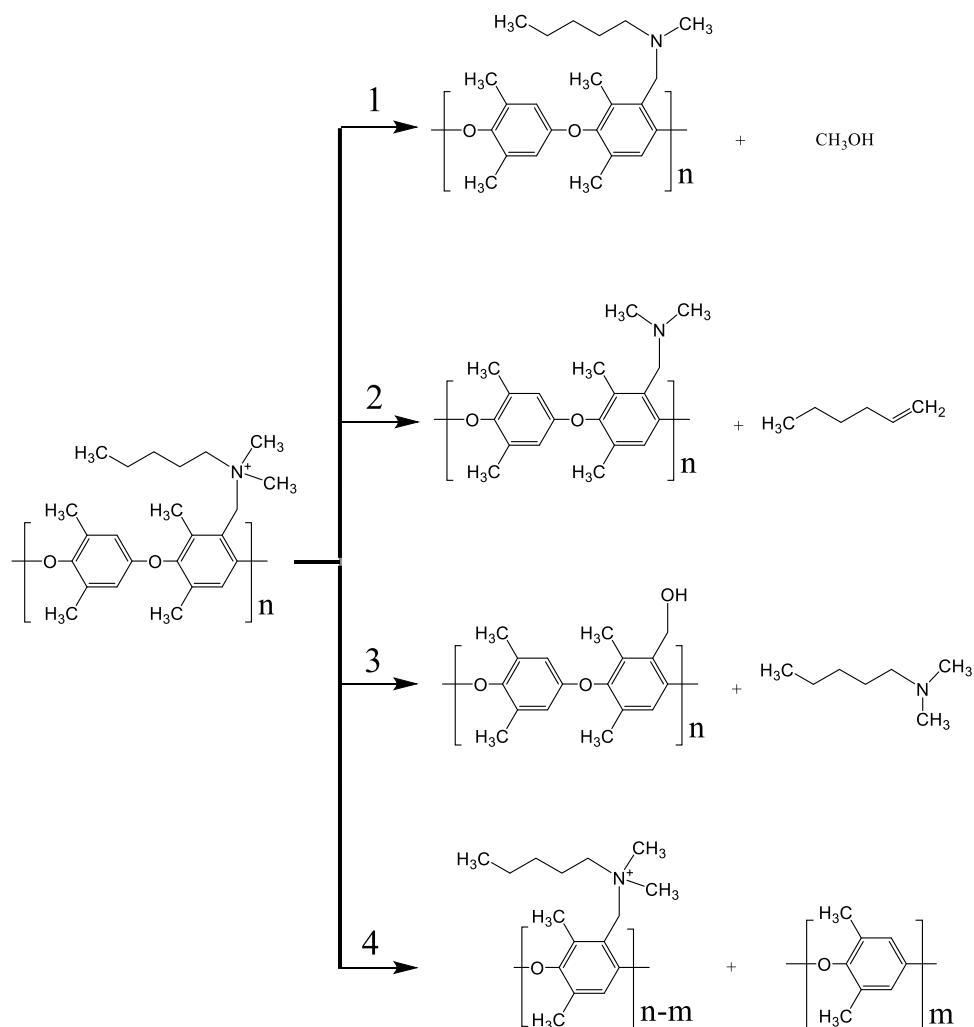
Figure 5: Four proposed chemical degradation pathways in PPO-2C1-C6 AEM. Reactions 1 and 2 correspond to methyl group losing and Hofmann elimination pathway degradations, respectively, both pathways were observed in ReaxFF simulations. Reactions 3 and 4 involve loss of the entire cationic group and backbone degradation and were not observed by ReaxFF.

In order to compare chemical degradation selectivity for the model membranes, Figure 6 illustrates residual number of cationic groups as a function of simulation time from the analysis of AEM chemical stability at 500 K. The higher temperature for these simulations was chosen to accelerate the degradation process. In this work, we averaged

three independent trajectories for each system to get reliable statistics. From Figure 6, it is clear that the PPO-3C3 shows the most chemically stable behavior. To quantify the stability for all systems, the residual number was fitted with two-parameter mono-exponential equation, which is given as $N(t)=N_0*exp[-(t-t_1)/t_2]$,[11] where N_0 is initial number of cationic groups (here, $N_0=80$), t is simulation time, t_1 and t_2 are initial decay time and exponential time constants, respectively. The lifetime can be estimated simply as t_1+t_2. The fitting curves are also displayed in Figure 6. Base on the fitting results, the lifetimes for PPO-3C1, PPO-2C1-EO, PPO-2C1-C6 and PPO-3C3 are 381.1, 539.3, 499.2 and 3546.2 ps, respectively. We should mention that the initial stage of the curve was used in our fitting, because the membrane degradation becomes much slower when the hydroxide ion concentration decreases during simulation due to its consumption. Our results demonstrate that PPO-3C1 is the least stable AEM while PPO-3C3 shows the best chemical stability, indicating that the larger size of alkyl side chain may block the OH⁻ approaching to the cation center.[10, 11] For the PPO-2C1-C6 and PPO-2C1-EO, although the long side chain can also stabilize the cation group in alkaline environment, it is not effective as the total substitution with long alkyl groups, such as PPO-3C3. In addition, The OH-anion residual number as a function of simulation time is also studied (shown in Figure S6) and we find the same membrane selectivity trends as that predicted from the view of cationic group number. It should be mentioned that although the simulated chemical degradation rate is much faster than the experiment result, due to employing accelerated ReaxFF simulations as discussed above, the ReaxFF predicts the reliable membrane degradation selectivity trends, as well as hydroxide dynamics. This can be proved from the comparison of the probability of OH-anion approaching the

cationic reaction center, showing the OH-anion in PPO-3C3 has a lower probability to react with cationic group compared to other membranes (see Figure S7). Moreover, our finding aligns well with experimental observations on similar membranes, which is also concluded that the membrane with large n-alkyl group has an increased stability.[5, 10] Furthermore, the focus of investigating degradation mechanism of PPO-based AEM is on the relative stability of different modifications patterns. From our study, we show a consistent trend in the stability of functional groups, which follows the order PPO-3C3 > PPO-2C1-C6 ≈ PPO-2C1-EO > PPO-3C1. It should be mentioned that the overall hydroxide ions concentration can also influence the stability of the AEMs, but this influence should minor in the comparison of present systems because all AEMs have similar volumes due to utilization of the PPO-based backbone, degree of functionalization, and hydration level.
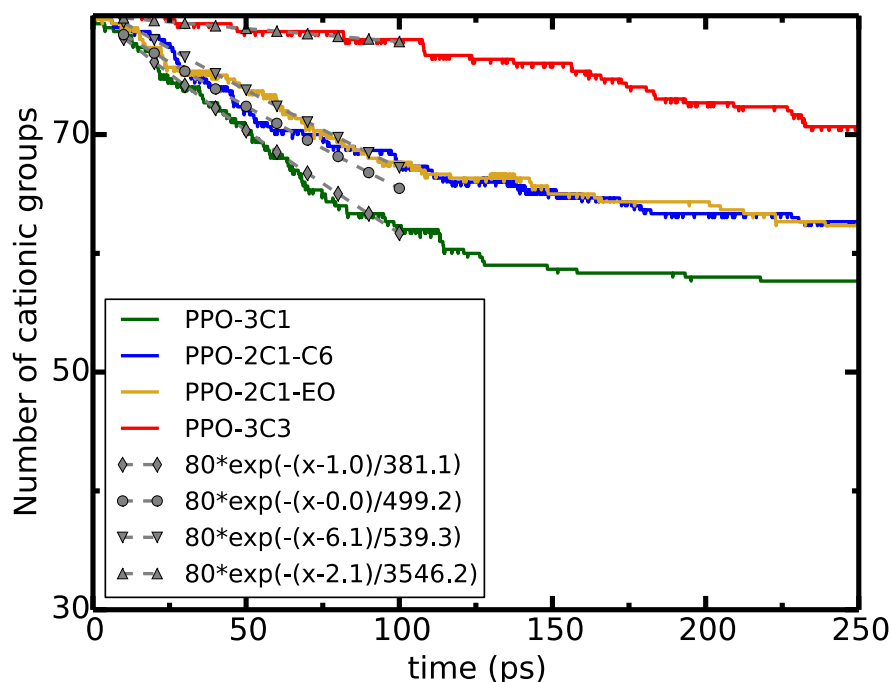
Figure 6: Time dependence of cationic group residual number in PPO-3C1, PPO-2C1-C6, PPO-2C1-EO and PPO-3C3 AEMs, as well as the two-parameter fitting curves.

From the study of conductivity and chemical stability selectivity of four AEM systems, we conclude that the PPO-3C3 with intermediate hydration level (i.e. around λ=10) might be the best candidate in the design of high performance AEMs, in which it shows a much better chemical stability, although it does reduce the OH$^-$ diffusion constant but the influence is not too much, as shown in the ReaxFF prediction. We should mention that on one hand it is known that increasing the water content is an alternative way to improve the conductivity and membrane chemical stability,[11] as also shown in Figure S8 for PPO-3C1. However, it is likely to lead to significant membrane swelling, which reduces the mechanical performance of AEMs as mentioned previously. On the other hand, lower water content often induces much poorer stability, as shown in Figure S8 and S9 for PPO-3C1 and PPO-3C3, respectively.

4 Conclusions

In this work, we combined APPLE&P and ReaxFF molecular dynamics simulations to study the proton transport and chemical stability of four anion exchange membranes (AEMs), namely PPO-3C1, PPO-2C1-C6, PPO-2C1-EO and PPO-3C3, which have the same backbones but different functionalized side chains. From the comparison of density, configuration of membrane, RDFs, as well as the morphology of water channel predicted with two force field calculations, we validated that the mapping between APPLE&P and ReaxFF structures is reliable. By studying the transport properties of AEMs we demonstrate the dominate contribution from Grotthuss hopping in the OH$^-$ overall diffusion, as well as its influence for water self-diffusion. The slow dynamics of water and OH$^-$ in APPLE&P arises from the stable OH-H$_2$O cluster and the necessity for OH$^-$ to lose its coordinating water molecules in order to diffuse through the bottlenecks in the water

channels, therefore creating a large kinetic barrier. However, accounting for the proton hopping in ReaxFF, the hydroxide diffuses much easier, without losing its hydration structure. As a result, the diffusion constants of OH^- are increased 100 times compared to APPLE&P prediction. Meanwhile, the diffusion of water is also enhanced about five times. We demonstrate that both hydrogen bonding between OH-anion and water and Grotthuss proton hopping can affect the water self-diffusion, and the presence of OH-anion leads to the slow water dynamics at high OH-concentration. From the comparison of OH^- diffusion in four AEMs predicted with APPLE&P and ReaxFF, we conclude that the Grotthuss mechanism makes the proton transport less depend on the morphology through water channels (at least for $\lambda=10$). In addition, the AEMs with well-defined water channel and enhanced nano-phase segregation show a relatively high OH^- transport efficiency, such as that in PPO-2C1-C6.

From the chemical degradation selectivity study of AEMs, we found that a large hydrophobic group attached to the quaternary ammonium cation group is very effective in the improvement of chemical stability of membrane, although it reduces the OH^- diffusion constant to a minor extent. For example, the lifetime of PPO-3C3 is ten times longer than that of PPO-3C1, and the OH^- diffusion in PPO-3C3 reduces less than 30% compared to other membranes. On the basis of our simulation results, we propose the PPO-3C3 with intermediate hydration level might be a good candidate for the design of high performance AEMs. Besides, the asymmetrical modification pattern (PPO-2C1-C6) is also a promising way to obtain membranes with improved conductivity with acceptable sacrifice of chemical stability. This study provides a guideline on how to improve the chemical stability of membrane in pursuit of conductivity of the AEM fuel cells.

With the strategy for combining the APPLE&P and ReaxFF simulations, the structural properties can be properly studied at the large length and time scales with APPLE&P simulations, while the charge transport and chemical stability selectivity of AEMs can be successfully predicted at a relatively short time-scale with ReaxFF simulations sampling more realistic electrochemical processes at the nanoscale. Furthermore, the degradation effect on the phase segregation of membranes can be studied by switching the ReaxFF back to APPLE&P simulations. It is intended for future works and we expect this back-and-forth strategy is a promising approach for the study of realistic materials at larger simulation scales.

Acknowledgments

Supporting Information

Electronic supplementary information (ESI) available. See DOI: xxx

Method of tracking OH-anion in ReaxFF simulations.

Method to calculate RDF, CN, diffusion constant, and water channel size distribution.

Time dependence of density and energy, MSDs of H_2O and OH^- in ReaxFF.

RDFs for small modeling system predicted with APPLE&P, standard and charge constrained ReaxFF simulations.

Time dependence of OH-anion residual number.

Comparison of coordination number of nitrogen-hydroxide in different AEMs.

Comparison of time dependence of OH-anion residual number in PPO-3C1 and PPO-3C3 with different hydration levels.

OH$^-$ hopping rate in different AEMs.

Lifetime of hydrogen bonds for OH$^-$(H$_2$O)$_n$ and H$_2$O(H$_2$O)$_n$.

Simulated ionic conductivities in different AEMs.

References

1. N. J. Robertson, H. A. Kostalik IV, T. J. Clark, P. F. Mutolo, H. D. Abruña and G. W. Coates, *J. Am. Chem. Soc.*, 2010, **132**, 3400-3404.
2. S. Lu, J. Pan, A. Huang, L. Zhuang and J. Lu, *Proc. Nat. Acad. Sci. USA*, 2008, **105**, 20611-20614.
3. M. Piana, M. Boccia, A. Filpi, E. Flammia, H. A. Miller, M. Orsini, F. Salusti, S. Santiccioli, F. Ciardelli and A. Pucci, *J. Power Sources*, 2010, **195**, 5875-5881.
4. Y. Leng, G. Chen, A. J. Mendoza, T. B. Tighe, M. A. Hickner and C.-Y. Wang, *J. Am. Chem. Soc.*, 2012, **134**, 9054-9057.
5. S. A. Nuñez, C. Capparelli and M. A. Hickner, *Chem. Mater.*, 2016, **28**, 2589-2598.
6. M. J. Hatch and W. D. Lloyd, *J. Appl. Polym. Sci.*, 1964, **8**, 1659-1666.
7. S. Chempath, J. M. Boncella, L. R. Pratt, N. Henson and B. S. Pivovar, *J. Phys. Chem. C*, 2010, **114**, 11977-11983.
8. S. Chempath, B. R. Einsla, L. R. Pratt, C. S. Macomber, J. M. Boncella, J. A. Rau and B. S. Pivovar, *J. Phys. Chem. C*, 2008, **112**, 3179-3182.
9. N. Li, Y. Leng, M. A. Hickner and C.-Y. Wang, *J. Am. Chem. Soc.*, 2013, **135**, 10124-10133.
10. A. L. Roy, C. D. Bruneau, K. Dietz, L. Zhu, G. A. Goenaga, A. Papandrew, M. A. Hickner, S. Foister and T. A. Zawodzinski, Meeting Abstracts, The Electrochemical Society: **2014**; 808-808.
11. W. Zhang and A. C. van Duin, *J. Phys. Chem. C*, 2015, **119**, 27727-27736.
12. N. Agmon, *Chem. Phys. Lett.*, 1995, **244**, 456-462.
13. G. Merle, M. Wessling and K. Nijmeijer, *J. Membr. Sci.*, 2011, **377**, 1-35.
14. M. Kumar and S. J. Paddison, *J. Mater. Res.*, 2012, **27**, 1982-1991.
15. H. Long, K. Kim and B. S. Pivovar, *J. Phys. Chem. C*, 2012, **116**, 9419-9426.
16. J. Pan, C. Chen, Y. Li, L. Wang, L. Tan, G. Li, X. Tang, L. Xiao, J. Lu and L. Zhuang, *Energy Environ. Sci.*, 2014, **7**, 354-360.
17. J. Lu, C. Miller and V. Molinero, *Phys. Chem. Chem. Phys.*, 2017, **19**, 17698-17707.
18. R. Devanathan, A. Venkatnathan, R. Rousseau, M. Dupuis, T. Frigato, W. Gu and V. Helms, *J. Phys. Chem. B*, 2010, **114**, 13681-13690.
19. R. Jorn, J. Savage and G. A. Voth, *Acc. Chem. Res.*, 2012, **45**, 2002-2010.
20. C. Chen, Y.-L. S. Tse, G. E. Lindberg, C. Knight and G. A. Voth, *J. Am. Chem. Soc.*, 2016, **138**, 991-1000.

21.   J. Cheng, G. He and F. Zhang, *Int. J. Hydrogen Energy*, 2015, **40**, 7348-7360.
22.   Y.-K. Choe, C. Fujimoto, K.-S. Lee, L. T. Dalton, K. Ayers, N. J. Henson and Y. S. Kim, *Chem. Mater.*, 2014, **26**, 5675-5682.
23.   D. R. Dekel, M. Amar, S. Willdorf, M. Kosa, S. Dhara and C. E. Diesendruck, *Chem. Mater.*, 2017, **29**, 4425-4431.
24.   A. C. van Duin, S. Dasgupta, F. Lorant and W. A. Goddard, *J. Phys. Chem. A*, 2001, **105**, 9396-9409.
25.   T. P. Senftle, S. Hong, M. M. Islam, S. B. Kylasa, Y. Zheng, Y. K. Shin, C. Junkermeier, R. Engel-Herbert, M. J. Janik, H. M. Aktulga, T. Verstraelen, A. Grama and A. C. van Duin, *npj Comput. Mater.*, 2016, **2**, 15011.
26.   K. Chenoweth, S. Cheung, A. C. van Duin, W. A. Goddard and E. M. Kober, *J. Am. Chem. Soc.*, 2005, **127**, 7192-7202.
27.   M. F. Russo, R. Li, M. Mench and A. C. van Duin, *Int. J. Hydrogen Energy*, 2011, **36**, 5828-5835.
28.   A. Strachan, A. C. van Duin, D. Chakraborty, S. Dasgupta and W. A. Goddard III, *Phys.l Rev. Lett.*, 2003, **91**, 098301.
29.   J. Wen, T. Ma, W. Zhang, G. Psofogiannakis, A. C. van Duin, L. Chen, L. Qian, Y. Hu and X. Lu, *Appl. Surf. Sci.*, 2016, **390**, 216-223.
30.   D. Dong, W. Zhang, A. C. van Duin and D. Bedrov, J. Phys. Chem. Lett., 2018, **9**, 825-829.
31.   T. P. Pandey, H. N. Sarode, Y. Yang, Y. Yang, K. Vezzù, V. Di Noto, S. Seifert, D. M. Knauss, M. W. Liberatore and A. M. Herring, *J. Electrochem. Soc.*, 2016, **163**, H513-H520.
32.   L. Liu, D. Li, Y. Xing and N. Li, *J. Membr. Sci.*, 2018, **564**, 428-435.
33.   B. V. Merinov and W. A. Goddard, *J. Membr. Sci.*, 2013, **431**, 79-85.
34.   S. S. Jang and W. A. Goddard, *J. Phys. Chem. C*, 2007, **111**, 2759-2769.
35.   D. Dong, X. Wei, J. B. Hooper, H. Pan and D. Bedrov, *Phys. Chem. Chem. Phys*, 2018, **20**, 19350-19362.
36.   D. Dong, J. B. Hooper and D. Bedrov, *J. Phys. Chem. B*, 2017, **121**, 4853-4863.
37.   W. Zhang and A. C. van Duin, *J. Phys. Chem. B*, 2018, **122**, 4083-4092.
38.   G. t. Te Velde, F. M. Bickelhaupt, E. J. Baerends, C. Fonseca Guerra, S. J. van Gisbergen, J. G. Snijders and T. Ziegler, *J. Computat. Chem.*, 2001, **22**, 931-967.
39.   A. Amel, S. B. Smedley, D. R. Dekel, M. A. Hickner and Y. Ein-Eli, *J. Electrochem. Soc.*, 2015, **162**, F1047-F1055.
40.   J. R. Varcoe, P. Atanassov, D. R. Dekel, A. M. Herring, M. A. Hickner, P. A. Kohl, A. R. Kucernak, W. E. Mustain, K. Nijmeijer and K. Scott, *Energy Environ. Sci.*, 2014, **7**, 3135-3191.
41.   S. Bhattacharya and K. E. Gubbins, *Langmuir*, 2006, **22**, 7726-7731.
42.   W. Zhang and A. C. van Duin, *J. Phys. Chem. B*, 2017, **121**, 6021-6032.
43.   H. N. Sarode, Understanding Ion and Solvent Transport in Anion Exchange Membranes under Humidified Condition. Colorado School of Mines. Arthur Lakes Library, 2015.
44.   S. Matsunaga, *Mol. Simulat.*, 2015, **41**, 913–917.
45.   A. M. A. Mahmoud, A. M. M. Elsaghier, K. Otsuji and K. Miyatake, *Macromolecules*, 2017, **50**, 4256-4266.
46.   C. G. Arges and V. Ramani, Proc. Nat. Acad. Sci. USA, 2013, **110**, 2490-2495.
47.   M. Marino and K. Kreuer, *ChemSusChem*, 2015, **8**, 513-523.

TOC Graphic